UC Santa Barbara

Title

Diffusiophoretic Focusing of Suspended Colloids

Authors

Shi, Nan
Nery-Azevedo, Rodrigo
Abdel-Fattah, Amr I
et al.

Peer reviewed

Diffusiophoretic Focusing of Suspended Colloids

Nan Shi,[1] Rodrigo Nery-Azevedo,[1] Amr I. Abdel-Fattah,[2] and Todd M. Squires[1,*]

[1]*Chemical Engineering department, University of California, Santa Barbara*
[2]*Saudi Aramco, Dhahran, Saudi Arabia*

Using a microfluidic system to impose and maintain controlled, steady-state multicomponent pH and electrolyte gradients, we present systems where the diffusiophoretic migration of suspended colloids leads them to focus at a particular position, even in steady-state gradients. We show that naively superpositing effects of each gradient may seem conceptually and qualitatively reasonable, yet is invalid due to the coupled transport of these multicomponent electrolytes. In fact, reformulating the classic theories in terms of the flux of each species (rather than local gradients) reveals rather stringent conditions that are necessary for diffusiophoretic focusing in steady gradients. Either particle surface properties must change as a function of local composition in solution (akin to isoelectric focusing in electrophoresis), or chemical reactions must occur between electrolyte species, for such focusing to be possible. The generality of these findings provides a conceptual picture for understanding, predicting, or designing diffusiophoretic systems.

Diffusiophoresis (DP) occurs when colloidal particles are driven into motion by solute concentration gradients [1–3]. In recent years, interest in DP has surged, particularly in new contexts such as polymer coating [4], membrane fouling [5,6], enhanced transport of particles into or out of dead-end pores [7,8], self-propelled particles [9,10], and the design of long-range "soluto-inertial" interactions in suspensions [11].

It is so common for DP to proceed up electrolyte gradients that a general sense has emerged that this is always the case, despite theory [12] and experiments [13] to the contrary. The fact that DP can occur in either direction raises the possibility of bidirectional DP and perhaps even focusing, akin to isoelectric focusing (IEF) in electrophoresis [14]. Thus far, however, DP focusing has only been reported in unsteady gradients [15,16].

Here, we demonstrate an unexpected DP focusing under steady-state gradients of multiple solutes. The focusing we observe differs from IEF, however, since particle zeta potentials are measured to be essentially constant for all experimental conditions. It is difficult to anticipate such focusing based on existing theories [1,12,17], which express DP migration in response to local concentration gradients. Because each ion species is electrostatically coupled to all others, a coupled set of transport equations must be solved to even determine these local gradients, as required by the theory.

Instead, we reexpress the DP theory to depend on the flux of each species (which is divergence free), rather than on local gradients (which are generally not). While it contains identical physics and makes identical predictions, this conceptual reformulation reveals that DP focusing can only be achieved in steady-state gradients under rather restrictive conditions: either the zeta potential of the particles must change appreciably with solute concentration (as occurs in IEF), or solute fluxes must diverge in solution, e.g. when consumed or produced by reactions. This new approach highlights conceptual surprises that remain still hidden in this classic field.

In the simplest case of binary and monovalent electrolyte gradients, the DP velocity takes the form [12,18]

$$U_{\mathrm{DP}} = \frac{3}{2} D_B \left(\tilde{\zeta}_p \beta + 4 \ln \cosh \frac{\tilde{\zeta}_p}{4} \right) \nabla \ln n_0^B, \qquad (1)$$

where $n_+^B + n_-^B = 2 n_0^B$ is the bulk electrolyte concentration, $\tilde{\zeta}_p = e\zeta_p/(k_B T)$ is the zeta potential scaled by the thermal potential, and $D_B = k_B T/(6\pi\eta\lambda_B)$ is the diffusivity of a sphere with radius of Bjerrum length $\lambda_B = e^2/(4\pi\epsilon k_B T)$. Two mechanisms—electrodiffusiophoresis (EDP) and chemi-phoresis (CP)—contribute to this expression. The first term, EDP, arises due to an electric field $E_s = (k_B T/e)\beta \nabla \ln n_0^B$ that is generated by the relaxation of gradients of ions with different diffusivity [Fig. 1(c)], parametrized by

$$\beta = \frac{D_+ - D_-}{D_+ + D_-}. \qquad (2)$$

EDP can occur either up or down ∇n_0^B, depending on the surface charge (ζ_p) and the direction of E_s (β). Anions diffuse more quickly ($\beta < 0$) in electrolytes like NaCl and NaOH, so that E_s is directed down the gradient [Fig. 1(c)-i], whereas cations diffuse more quickly in KIO_3 and HCl, so that E_s points up the gradient [Fig. 1(c)-ii]. In special cases (e.g. KCl), $D_+ \approx D_-$, so that $|\beta| \ll 1$ and EDP is negligible. The second term in Eq. (1) represents chemi-phoresis and corresponds to entropic forces on the electric double layer
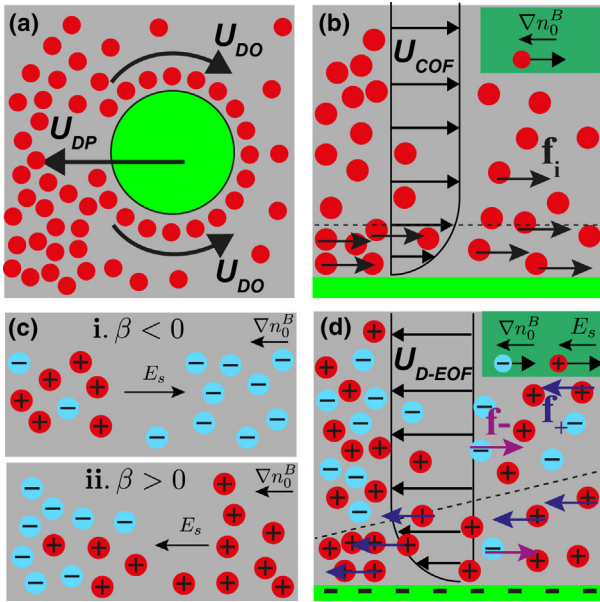
FIG. 1.   (a) A concentration gradient drives a diffusio-osmotic slip velocity U_{DO} along the surface of a suspended particle, causing diffusiophoretic migration with velocity U_{DP}. (b) A gradient ∇n_0^B forces excess ions within the electric double layer (dashed line) near a surface (green) into chemi-osmotic slip, with velocity U_{COF}. (c) Gradients of ions with different diffusivities, defined by β (2), establish a spontaneous electric field $E_s \propto \beta \nabla n_0^B$ to prevent large-scale charge separation. (d) Spontaneous fields E_s drive electrodiffusioosmotic slip (U_{E-DOF}) in a direction depending on surface charge ($\tilde{\zeta}_p$) and ion diffusivity difference (β). Here, the E_s established by fast cations ($\beta > 0$) points up the gradient, forcing the positively charged EDL around a negatively charged surface ($\zeta < 0$) into E-DOF flow up the gradient.

(EDL) that induce chemi-osmotic flows (COF) down the electrolyte gradient [Fig. 1(b)], thereby driving *CP* up the gradient. Ultimately, DP can occur either up or down ∇n_0^B, depending on the direction of EDP, and its magnitude relative to *CP*.

On the experimental side, it has been difficult to systematically measure DP mobilities, although methods have been improved from early techniques involving membrane deposition [2] or stop-flow diffusion cells [19] to microfluidic devices made in agarose gels [20]. We have recently developed a microfluidic system that allows systematic and quantitative measurement of DP mobilities [13]. Integrated hydrogel microwindow membranes [21] enable a wide range of solute gradients to be imposed without generating convective flows, and particle DP to be visualized directly and measured quantitatively.

We begin with DP migration of fluorescent polystyrene (PS) particles (diameter 0.52 μm, Bangs Laboratories, FS03F) under single-component pH gradients, established with gradients of NaOH (basic) and HCl (acidic), respectively. We measured ζ for these particles to remain fairly constant (-55 ± 6 mV) in the pH range between 4 and 10 relevant to these experiments [22].

In NaOH, OH$^-$ diffuses faster than Na$^+$ ($D_{Na^+} = 1.3 \times 10^{-9}$ m^2/s and $D_{OH^-} = 5.0 \times 10^{-9}$ m^2/s), giving $\beta = -0.6$ [26]. NaOH gradients thus generate spontaneous electric fields pointing down ∇[NaOH] [Fig. 1(c)-i], which for $\zeta_p < 0$ drives E-DOF down NaOH gradients, like COF. PS particles move diffusiophoretically in the opposite direction, up ∇[NaOH] [Fig. 2(a)].

In HCl, by contrast, H$^+$ diffuses much faster than Cl$^-$ ($D_{H^+} = 9.3 \times 10^{-9}$ m^2/s and $D_{Cl^-} = 2.0 \times 10^{-9}$ m^2/s), giving $\beta = 0.65$ [26]. E_s thus points up HCl gradients [Fig. 1(c)-ii], driving E-DOF slip up ∇[HCl] [Fig. 1(d)], opposite to COF. In fact, β is so large for HCl that EDP dominates, driving DP down ∇[HCl] [Fig. 2(b)].

Diffusiophoretic trajectories under each gradient are visualized by overlaying particle positions at 0.1 s time intervals [insets, Fig. 2(c)]. Particles migrate down HCl gradients, yielding particle-depleted regions on the high [HCl] side, and vice versa for NaOH. DP velocities measured in both NaOH and HCl [Fig. 2(c)] agree quantitatively with Eq. (1), using $\zeta_p \approx -55$ mV, as measured independently (see Supplemental Material [22]). Moreover, DP is notably smaller under ∇[HCl] than ∇[NaOH], as expected from the fact that EDP and *CP*
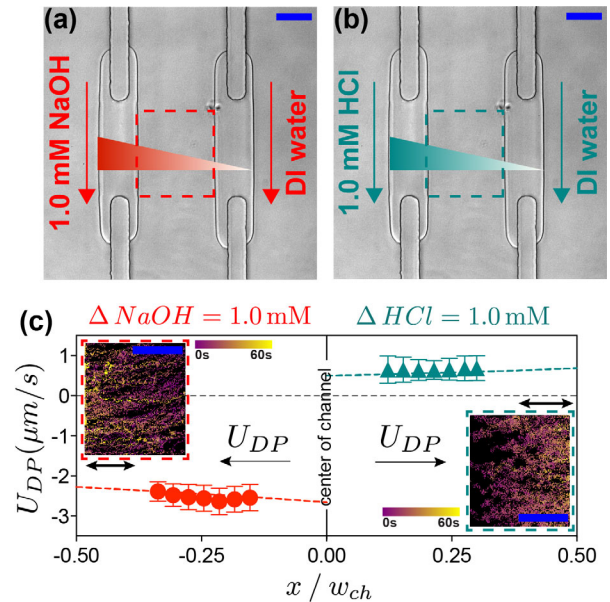

FIG. 2.   Diffusiophoresis under (a) basic [NaOH] and (b) acidic [HCl] gradients. High- and low-concentration solutions flow in the left and right reservoir channels, respectively, to create steady-state gradients across the sample channel (dashed box). (c) Measured diffusiophoretic velocities (markers) at different positions within gradients compare well with the classic theory [dashed lines, from Eq. (1)]. Streakline images clearly show DP motions up and down NaOH and HCl gradients, respectively. DP velocities are greater in NaOH gradients than in HCl gradients, as expected because EDP and *CP* are oppositely directed in HCl gradients, but aligned in NaOH gradients. All scale bars are 50 μm.

are counterdirected under HCl gradients but aligned for ∇[NaOH].

Having established qualitative and quantitative understanding of DP in single component gradients, we now turn to multicomponent gradients. Counterposed NaOH and HCl gradients establish even stronger pH gradients [Fig. 3(a)], driving PS particles from high [HCl] to high [NaOH], consistent with the down-∇[HCl] and up-∇[NaOH] DP observed in Fig. 2. Counterposing NaCl gradients against these HCl-NaOH gradients, however, results in an unexpected DP focusing [Figs. 3(b) and 3(c)]. The focusing position moves towards higher [NaCl] as ∇[NaCl] increases, and ultimately vanishes for ∇[NaCl] strong enough to overwhelm ∇pH [Fig. 3(d)]. Figure S2 [22] quantifies the DP focusing strength with an effective "pseudopotential" ϕ_{PS} that would give rise to the concentration profiles in Figs. 3(b) and 3(c), revealing
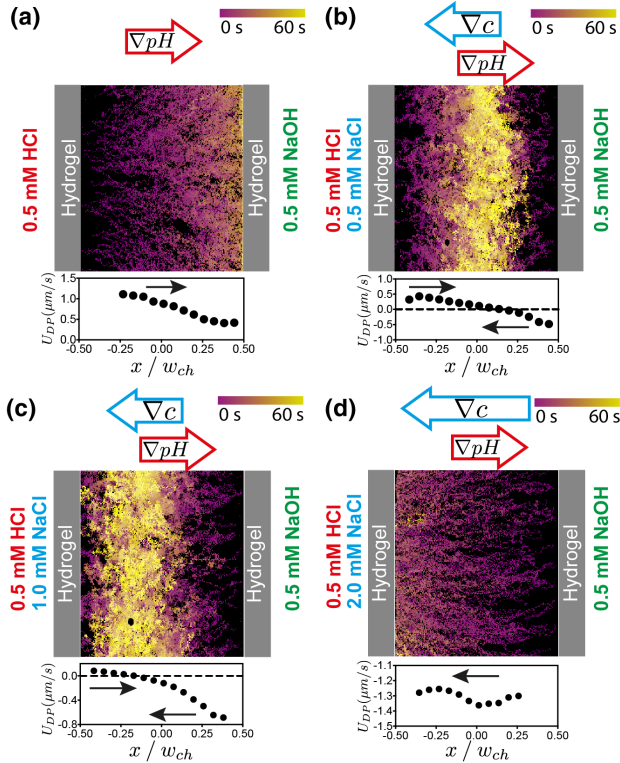

FIG. 3. Diffusiophoresis under combined pH and salt gradients. (a) Counter-posed NaOH and HCl gradients are created by flowing 0.5 mM NaOH and 0.5 mM HCl solution separately in two reservoir channels, establishing a gradient in pH from 3.3 (left) to 10.7 (right), within which DP proceeds monotonically to right as expected from Fig. 2. (b)–(d) NaCl gradients of different strengths are counter-posed against the HCl-NaOH pH gradient. (b) Streakline images reveal unexpected focusing at a location that shifts toward higher [NaCl] as the NaCl gradient strength increases (c). (d) Sufficiently strong NaCl gradients overwhelm pH gradients so that DP migration always proceeds up NaCl gradients. Insets show measured DP velocities vs position x (and thus composition).

pseudopotential "wells" 2–6 k_BT deep. Because DP is a strictly nonequilibrium phenomenon; however, any such pseudopotential ϕ_{PS} should be taken only as a guide, rather than a physically or conceptually intrinsic quantity.

One might anticipate the sequence in Figs. 3(a)–(d), based on a straightforward, intuitive superposition of the DP associated with each individual gradient. This agreement is fortuitous, however, because gradients do not simply superpose in multicomponent electrolytes, owing to the electrostatic coupling between electrolytes that generates E_s. In fact, without explicitly solving for the ion concentration profiles, one cannot determine the concentration gradients required to use classic DP theories [12], or their generalization to multicomponent electrolytes [17].

To address this gap, we reformulate the standard theory so that the DP velocity is expressed in terms of the flux of each ion species—each of which obeys a macroscopic conservation equation—rather than local concentration gradients, which do not. Our result gives identical predictions to existing theories [12,17] in the appropriate limits; however, its form allows concrete predictions to be made based on macroscopic conservation principles.

We derive the diffusio-osmotic flow over a surface as a sum of contributions from each species i, following [27]. In the thin-EDL limit, the phoretic mobility of a particle is equal and opposite to the osmotic slip mobility [28]. The EDL around a charged surface is comprised of a relative excess or deficit of each species, $\Delta n_i(z) = n_i - n_i^B$. Each ion experiences a force given by the gradient of its chemical potential, $f_i = -\nabla \mu_i$, so that the net body force within the EDL (assumed thin) is

$$\vec{f} = \sum_i -\nabla \mu_i^B \Delta n_i. \qquad (3)$$

The surrounding fluid responds according to the forced Stokes equations,

$$0 = \eta \frac{\partial^2 u_x}{\partial z^2} - \sum_{i=1}^{N} \Delta n_i(z) \nabla \mu_i^B, \qquad (4)$$

where u_x is the velocity parallel to the particle surface. Integrating Eq. (4) twice from the particle surface ($z = 0$) to the bulk solution ($z \to \infty$) yields an expression for the osmotic "slip" velocity between the bulk fluid and the particle surface [28],

$$U^s = \sum_i (-\nabla \mu_i^B) M_i = -U_{DP}, \qquad (5)$$

where M_i is the contribution of species i to the DOF mobility,

$$M_i = \frac{1}{\eta} \int_0^\infty z \Delta n_i(z) dz. \qquad (6)$$

In the thin-EDL limit, the DP mobility is simply negative the DO mobility [28].

While the mobility integrals (6) are general, they can be performed analytically for binary, monovalent electrolytes, using the Guoy-Chapman EDL, to give

$$M_{\pm}^{\mathrm{GC}} = \frac{\epsilon}{e\eta}\frac{k_B T}{2e}\left(\mp\tilde{\zeta}_p + 4\ln\cosh\frac{\tilde{\zeta}_p}{4}\right) \equiv -M_{\pm}^{\mathrm{DP}}. \quad (7)$$

Multicomponent (but monovalent) electrolytes have the same EDL structure, giving contributions

$$M_i = \frac{n_i}{n_0^B}M_{\pm}^{\mathrm{GC}}, \quad (8)$$

where $\pm$ is chosen according to the valence of species i. Equations (5)–(8) reproduce conventional DP theories, as can be seen by inserting $\mu_i = \pm e\phi + k_B T\ln n_i$, and using the standard expression for E_s. The advantage of the current approach, however, is that the chemical potential gradients can be related to species fluxes, via

$$j_i^B = (-\nabla\mu_i^B)\frac{D_i}{k_B T}n_i^B. \quad (9)$$

Solving for $\nabla\mu_i^B$ and inserting into (5) along with (8) yields a remarkable formula for the DP velocity in multi-component electrolyte gradients,

$$U_{\mathrm{DP}} = \frac{k_B T}{n_0^B}\left(M_+^{\mathrm{DP}}\sum_+\frac{j_i^B}{D_i} + M_-^{\mathrm{DP}}\sum_-\frac{j_i^B}{D_i}\right). \quad (10)$$

To actually determine the species fluxes j_i^B—e.g. to compute specific DP velocities—one must solve the coupled set of ion transport equations (just like for ∇n_i^B). Even without determining the individual species fluxes j_i^B, however, stringent conditions for DP focusing arise due to the constraints imposed by macroscopic conservation, which would not be evident from conventional DP theory.

For focusing to occur in steady-state gradients, U_{DP} must change sign across the focusing point, from positive to negative. Of the variables that impact U_{DP} in (10), however, only n_0^B, $M_{\pm}(\zeta_p)$, and j_i^B may potentially vary with position. Of these, $M_{\pm}(\zeta_p)$ only changes if ζ_p does (e.g. via charge regulation due to local pH), as occurs in electrophoretic IEF. In our experiments, however, $\tilde{\zeta}_p \approx -2.1$ over all conditions, ruling out this mechanism for focusing. While n_0^B generally does change in such systems, it appears as a prefactor and cannot reverse U_{DP}. Finally, basic conservation laws almost always require $\nabla\cdot j_i^B = 0$, which might appear to render focusing impossible.

Species fluxes with nonzero divergence can occur, however, if those species react in solution. In the present experiments, for example, H^+ and OH^- react to form H_2O. This reaction introduces abrupt changes in j_{H^+} and j_{OH^-}: on

the acidic side, j_{OH^-} is zero, while j_{H^+} is nonzero and divergence free, and vice versa for the basic side. Different fluxes thus enter (10) on the acidic and basic sides of the reaction, giving

$$U_{\mathrm{DP}}^L = \frac{k_B T}{n_L^B}\left\{\left(\frac{j_{\mathrm{Na}^+}}{D_{\mathrm{Na}^+}} + \frac{j_{\mathrm{H}^+}}{D_{\mathrm{H}^+}}\right)M_+^{\mathrm{DP}} + \frac{j_{\mathrm{Cl}^-}}{D_{\mathrm{Cl}^-}}M_-^{\mathrm{DP}}\right\},$$

$$U_{\mathrm{DP}}^R = \frac{k_B T}{n_R^B}\left\{\frac{j_{\mathrm{Na}^+}}{D_{\mathrm{Na}^+}}M_+^{\mathrm{DP}} + \left(\frac{j_{\mathrm{OH}^-}}{D_{\mathrm{OH}^-}} + \frac{j_{\mathrm{Cl}^-}}{D_{\mathrm{Cl}^-}}\right)M_-^{\mathrm{DP}}\right\}. \quad (11)$$

The change in u_{DP} across the reaction zone can indeed cause focusing.

Applying the strict requirement for DP focusing (i.e. $U_{\mathrm{DP}}^L > 0$ and $U_{\mathrm{DP}}^R < 0$) would require all ion fluxes to be determined. Even without doing so, however, strong constraints on conditions for focusing can be determined by imposing a necessary (but not sufficient) condition, that $U_{\mathrm{DP}}^L > U_{\mathrm{DP}}^R$. Because n_0^B is continuous across the reaction zone, nonreactive species fluxes cancel, leaving

$$\frac{j_{\mathrm{H}^+}}{D_{\mathrm{H}^+}}M_+^{\mathrm{DP}}(\zeta_p) > \frac{j_{\mathrm{OH}^-}}{D_{\mathrm{OH}^-}}M_-^{\mathrm{DP}}(\zeta_p). \quad (12)$$

Reaction stoichiometry requires j_{H^+} and j_{OH^-} to be equal and opposite, yielding

$$\frac{D_{\mathrm{OH}^-}}{D_{\mathrm{H}^+}} < -\frac{M_-^{\mathrm{DP}}(\zeta_p)}{M_+^{\mathrm{DP}}(\zeta_p)} = \frac{\tilde{\zeta}_p + 4\ln\cosh\frac{\tilde{\zeta}_p}{4}}{\tilde{\zeta}_p - 4\ln\cosh\frac{\tilde{\zeta}_p}{4}}. \quad (13)$$

Equation (13) represents a simple constraint on the maximum ratio of ion diffusivities that can possibly focus particles with $\tilde{\zeta}_p$. Whether focusing actually occurs depends on all ion fluxes—e.g. particles focus under the fluxes imposed in Figs. 3(b) and 3(c), but not for those in Figs. 3(a) and 3(d). Focusing is impossible, however, if (13) is not satisfied. For example, $D_{\mathrm{OH}^-}/D_{\mathrm{H}^+} = 0.54$, which is indeed lower than the critical ratio of 0.6 calculated for $\tilde{\zeta}_p = -2.1$. By contrast, particles with this ζ_p could not be focused using counterposed NH_4^+ and OH^- gradients, which react to form NH_3 and $\mathrm{H}_2\mathrm{O}$, no matter what other ion fluxes were superposed, because $D_{\mathrm{NH}_4^+} = 1.9\times10^{-9}$ m²/s [26], giving $D_{\mathrm{OH}^-}/D_{\mathrm{NH}_4^+} = 2.5$, which significantly exceeds the threshold 0.6. Divergent species fluxes arise under a wide variety of reactions—ionic, dissociative, or even aggregative (e.g. formation of surfactant micelles)—and therefore may give rise to focusing.

Our microfluidic system enables complex, multi-component gradients to be established and maintained in otherwise quiescent solutions. With these capabilities, our experiments enable diffusiophoretic mobilities to be measured quantitatively—much like ζ_p can be measured routinely via electrophoresis—and reveal qualitative surprises. In particular, the diffusiophoretic focusing reported

here does follow from extensions of the classic theory, yet would have been very difficult to observe using classic (membrane deposition or stop-flow) techniques. These observations highlight the nontrivial consequences of coupled, multicomponent fluxes. By reformulating the classic DP theory to account for each species' contribution to the DP migration, and moreover by expressing the migration in terms of bulk fluxes of each species, restrictive, but clear, conditions for DP focusing can be determined. The essential role of the chemical reaction, in particular, would not have been apparent *a priori*, but provides important insight for future design and understanding of colloids in nonequilibrium environments.

---

[*]Corresponding author.
squires@engineering.ucsb.edu

[1] B. V. Deryaguin, S. S. Dukhin, A. A. Korotkova, and S. S. K. A. A. D. B. V. Dukhin, Kolloidn. Zh. **23**, 53 (1961).

[2] M. M.-J. Lin and D. C. Prieve, J. Colloid Interface Sci. **95**, 327 (1983).

[3] J. P. Ebel, J. L. Anderson, and D. C. Prieve, Langmuir **4**, 396 (1988).

[4] D. C. Prieve, R. E. Smith, R. A. Sander, and H. L. Gerhart, J. Colloid Interface Sci. **71**, 267 (1979).

[5] R. Guha, X. Shang, A. L. Zydney, D. Velegol, and M. Kumar, J. Membr. Sci. **479**, 67 (2015).

[6] D. Florea, S. Musa, J. M. R. Huyghe, and H. M. Wyss, Proc. Natl. Acad. Sci. U.S.A. **111**, 6554 (2014).

[7] A. Kar, T.-Y. Chiang, I. O. Rivera, A. Sen, and D. Velegol, ACS Nano **9**, 746 (2015).

[8] S. Shin, E. Um, B. Sabass, J. T. Ault, M. Rahimi, P. S. Warren, and H. A. Stone, Proc. Natl. Acad. Sci. U.S.A. **104**, 20167 (2015).

[9] B. Abécassis, C. Cottin-Bizonne, C. Ybert, A. Ajdari, and L. Bocquet, New J. Phys. **11**, 075022 (2009).

[10] J. J. McDermott, A. Kar, M. Daher, S. Klara, G. Wang, A. Sen, and D. Velegol, Langmuir **28**, 15491 (2012).

[11] A. Banerjee, I. Williams, R. N. Azevedo, M. E. Helgeson, and T. M. Squires, Proc. Natl. Acad. Sci. U.S.A. **113**, 8612 (2016).

[12] J. L. Anderson, M. E. Lowell, D. C. Prieve, J. L. Anderson, J. P. Ebel, and M. E. Lowell, J. Fluid Mech. **148**, 247 (1984).

[13] J. S. Paustian, C. D. Angulo, R. Nery-Azevedo, N. Shi, A. I. Abdel-Fattah, and T. M. Squires, Langmuir **31**, 4402 (2015).

[14] M. Prats, Biochem. Educ. **20**, 111 (1992).

[15] B. Abécassis, C. Cottin-Bizonne, C. Ybert, A. Ajdari, and L. Bocquet, Nature Materials **7**, 785 (2008).

[16] J. Palacci, C. Cottin-Bizonne, C. Ybert, and L. Bocquet, Soft Matter **8**, 980 (2012).

[17] T.-Y. Chiang and D. Velegol, J. Colloid Interface Sci. **424**, 120 (2014).

[18] S. Dukhin and B. Derjaguin, in *Surface and Colloid Science*, edited by E. Matijevic (John Wiley and Sons, New York, 1974), Vol. 7.

[19] P. O. Staffeld and J. A. Quinn, J. Colloid Interface Sci. **130**, 88 (1989).

[20] J. Palacci, B. Abécassis, C. Cottin-Bizonne, C. Ybert, and L. Bocquet, Phys. Rev. Lett. **104**, 138302 (2010).

[21] J. S. Paustian, R. N. Azevedo, S.-T. B. Lundin, M. J. Gilkey, and T. M. Squires, Phys. Rev. X **3**, 041010 (2013).

[22] See Supplemental Material at http://link.aps.org/supplemental/10.1103/PhysRevLett.117.258001, which includes Refs. [13, 23-25], for zeta potential measurement and image analysis of colloid migration.

[23] Y. Xia and G. M. Whitesides, Annu. Rev. Mater. Sci. **28**, 153 (1998).

[24] D. Bartolo, G. Degré, P. Nghe, and V. Studer, Lab Chip **8**, 274 (2008).

[25] S. T. Wereley and C. D. Meinhart, Annu. Rev. Fluid Mech. **42**, 557 (2010).

[26] E. L. Cussler, *Diffusion* (Cambridge University Press, Cambridge, United Kingdom, 1997).

[27] T. M. Squires, in *Fluids, Colloids and Soft Materials: An Introduction to Soft Matter Physics*, edited by A. F.-N. A. M. Puertas (John Wiley & Sons, Inc, New York, 2016), Chap. 5, pp. 59–80.

[28] J. L. Anderson, Annu. Rev. Fluid Mech. **21**, 61 (1989).